# Cyclopia and defective axial patterning in mice lacking *Sonic hedgehog* gene function

**Chin Chiang*†, Ying Litingtung*†, Eric Lee*, Keith E. Young†, Jeffrey L. Corden†, Heiner Westphal* & Philip A. Beachy†**

* Laboratory of Mammalian Genes and Development, National Institute of Health, Bethesda, Maryland 20892, USA
† Howard Hughes Medical Institute, Department of Molecular Biology and Genetics, Johns Hopkins University School of Medicine, Baltimore, Maryland 21205, USA

**Targeted gene disruption in the mouse shows that the *Sonic hedgehog* (*Shh*) gene plays a critical role in patterning of vertebrate embryonic tissues, including the brain and spinal cord, the axial skeleton and the limbs. Early defects are observed in the establishment or maintenance of midline structures, such as the notochord and the floorplate, and later defects include absence of distal limb structures, cyclopia, absence of ventral cell types within the neural tube, and absence of the spinal column and most of the ribs. Defects in all tissues extend beyond the normal sites of *Shh* transcription, confirming the proposed role of Shh proteins as an extracellular signal required for the tissue-organizing properties of several vertebrate patterning centres.**

EXPERIMENTAL vertebrate embryology has demonstrated the capacity of certain tissues to influence the pattern of cell types within adjacent embryonic tissues, presumably through the action of secreted signalling molecules. Vertebrate gene products related to that of *hedgehog* (*hh*), first characterized as encoding a secreted protein signal in *Drosophila*[1,2], have emerged as the molecules likely to be responsible for several such patterning activities. The most-studied member of this multi-gene family in vertebrates is *Sonic hedgehog* (*Shh*), which has been isolated from many species, including mouse, chicken, rat, frog, fish and human[3–9]. These initial studies of *Shh* gene expression demonstrated an association with embryonic structures such as the notochord, the floorplate of the neural tube, and the posterior margin of tetrapod limb buds, all of which are known to have organizing properties in transplantation and grafting experiments.

The expression of *Shh* at these locations and the secretion of the Shh protein suggest that it is involved in patterning. Support for this suggestion comes from experimental expression or placement of the Shh protein at ectopic locations in embryos, and from treatment of explanted embryonic target tissues with purified protein. Thus, for example, cells infected with a retrovirus carrying the chicken *Shh* gene or transfected with a mouse *Shh* expression construct are capable of inducing mirror-image limb-digit duplications when grated to the anterior margin of the embryonic chick limb bud[4,7]; similar duplications resulted from grafting of beads impregnated with purified protein to the anterior limb bud margin[10]. In the neural tube, ectopic expression of *Shh* promotes the expression of genes normally expressed at or near the ventral midline, analogous to the effects of ectopic notochord grafts[3,5,6,11]. These ventral patterning effects extend to the brain and eyes[9,12–14] and to the somites, where *Shh* seems to promote formation of sclerotome ventrally and to repress more dorsal somite fates[15,16]. Treatment of neural plate and presomitic mesoderm explants with purified protein also induced cell type-specific genes, with floorplate markers induced at high concentrations and motor neuron and sclerotome markers at lower concentrations[16–18].

These experimental approaches demonstrated a potential role for *hh* activity in several aspects of embryonic patterning. However, because multiple vertebrate *hh* genes display similar signalling activities[8,9,14], these studies did not establish a unique requirement for *Shh*. To examine more directly the role of *Shh* in normal embryonic patterning and to search for other as-yet unidentified patterning activities, we undertook the targeted mutagenesis of the *Shh* gene in the mouse.

## Targeted disruption of *Shh*

Mice homozygous for a disrupted *Shh* gene were generated by using homologous recombination in embryonic stem (ES) cells (Fig. 1*a*). In the targeting vector, a PGK-*neo* cassette replaced exon 2 and portions of the flanking introns, leaving coding sequences that would result in a truncated protein (Fig. 1*a*). This deletion causes a loss of 97 of the 198 residues within the N-terminal product of *Shh* autocatalytic processing, including most of the $\alpha + \beta$ sandwich (both of the $\alpha$-helices and the central four of six $\beta$-strands) that forms the core of the N-terminal domain structure[19]. This domain is responsible for all Shh signalling activity, including the induction of a variety of ventral neural and somite cell types, and also the induction and patterning of distal limb structures[9,10,12,17,18,20,21]. The targeting vector also contains two thymidine kinase genes at positions flanking the *Shh* genomic region for counter-selection of ES cells.

Southern analysis of 200 ES clones selected for thymidine kinase and neo resistance revealed 19 with a 5.5-kb *Eco*RI fragment, indicative of the deletion of exon 2 (data not shown). Chimaeric mice were generated by blastocyst injections from six independent ES cell lines containing the disrupted *Shh* allele. Two *Shh* mutant lines were then established through germline transmission of ES clones 199 and 184. Genotypes of the progeny were determined using Southern and polymerase chain reaction (PCR) analyses (Fig. 1*b*, *c*). Heterozygous mice seem normal, but only two homozygous mutant stillborn pups from more than a thousand progeny were recovered from crosses of $Shh^{+/-}$ individuals. Genotypic analysis of embryos from 7.5 to 18.5 days post-coitum (d.p.c.) showed no obvious deviation from the expected Mendelian ratio (data not shown), indicating that most *Shh* mutant embryos die at or just before birth, with probable rapid cannibalization of stillborn pups.

## Abnormal anatomy and histology

The earliest detectable morphological defects occur in the future forebrain region of homozygous mutant embryos at embryonic day 9.5 (E8.5). The cephalic neural tube at this stage has not yet closed, and the neural folds are quite extensive with well-defined lips that extend to a clearly defined ventral midline. In *Shh* mutant

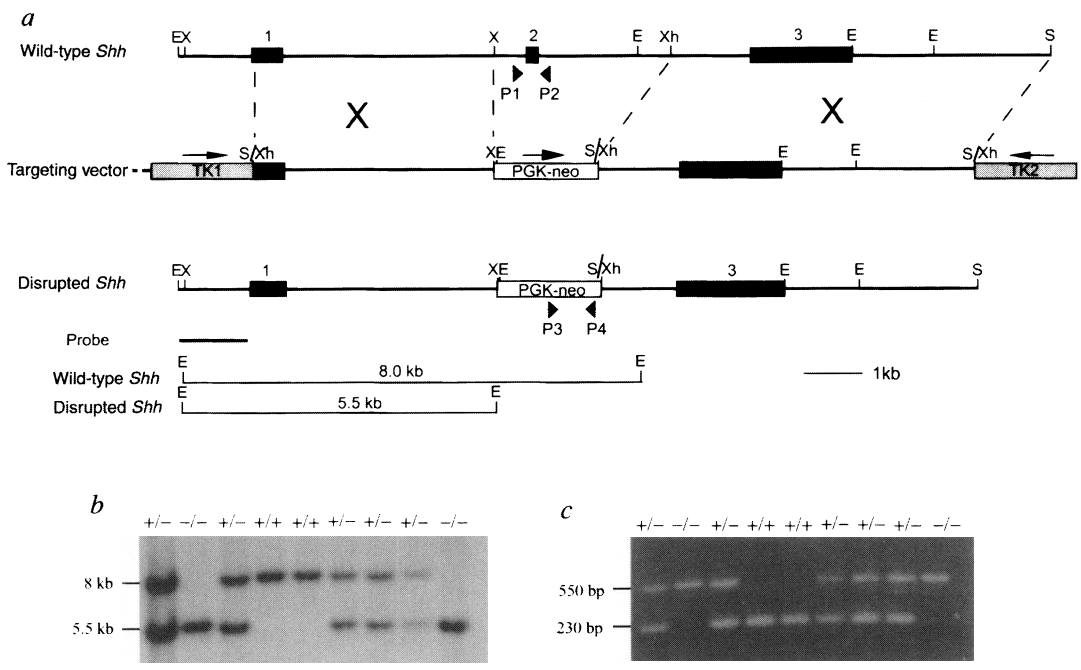


FIG. 1 Disruption of the *Shh* gene by targeted recombination. *a*, Maps of the wild-type *Shh* locus, the targeting vector, and the disrupted *Shh* allele. Relative positions of the three *Shh* exons are indicated by black boxes. The map of the targeting vector shows the replacement of exon 2 and flanking genomic sequences by the Neomycin gene (*neo*), and the locations of two flanking HSV thymidine kinase genes (TK). Arrowheads denote the sites within the wild-type and the disrupted *Shh* alleles from which PCR primers are derived; lines at the bottom indicate expected sizes for *Eco*RI-generated fragments detected with a 5′ flanking genomic probe from wild-type and disrupted *Shh* alleles. *b*, Southern analysis of DNA from individual embryos, the progeny of a heterozygous mating. Sizes of the wild-type and the targeted alleles are indicated by 8-kb and 5.5-kb hybridizing bands, respectively. *c*, PCR analysis of the same DNA samples as in *b*. The 230-bp (primers P1 and P2) and 550-bp (primers P3 and P4) amplification products are specific to exon 2 of the wild-type *Shh* and to the *neo* gene within the disrupted *Shh* locus, respectively.

embryos, however, the midline is indistinct (compare Fig. 2*a* with Fig. 2*b*; arrow), the ventral lips of the cephalic folds are fused, and the normally separate optic vesicles appear instead as a continuous single vesicle protruding at the ventral midline. The cephalic defects in *Shh* mutant embryos become even more apparent when the neural tube closes, with an overall reduction in size of the brain and spinal cord. This is especially apparent at the mesencephalic/diencephalic junction of E9.5 embryos, where floor and roof of the neural tube are almost in contact with each other (arrowhead in Fig. 2*c*). By E11.5, as normal brain structures become more prominent, the small size and defects in the presumptive midbrain and forebrain of *Shh* mutant embryos can be clearly observed (Fig. 2*d*); the most obvious specific defect is the absence of externally visible lateral eye structures. By E15.5 (Fig. 2*e*), *Shh* mutant embryos exhibit severe growth retardation throughout most of the embryo and lack the distinct forelimb and hindlimb structures found in their normal littermates. In addition, relative growth deficits in the forebrain and in craniofacial structures are so extreme that normal facial features such as the eyes, nose and oral structures are not identifiable, and the sole remaining external feature of the mutant head is a proboscis-like extension that protrudes from the rostral midline. Gross inspection and preliminary histological analysis of the internal organs of E18.5 mutant embryos revealed abnormalities of heart, lung, kidney and foregut development (C.C. *et al.*, unpublished data), although asymmetry of early heart looping and internal organ situs appeared normal in all mutant embryos examined.

As noted above, bilateral eye structures are not observed in *Shh* mutant embryos at any stage of development, and the optic vesicle is single and continuous from its earliest appearance at ~E8.5. At E9.5, expression of the gene *microphthalmia* can be detected throughout this vesicle (Fig. 2*f*, *g*), suggesting that these cells are precursors of pigmented retinal epithelium[22]. Indeed, by E15.5 an accumulation of pigmented tissue is found consistently at the base of and just under the proboscis of these mutant embryos (Fig. 2*e*, arrowhead). In addition, expression of *Fgf-8* at E10.5 revealed a single nasal pit at the midline instead of the bilateral pits normally observed (compare Fig. 2*h* with Fig. 2*i*). Cross-sections of the neural tube at the level of the spinal cord and at other axial levels also revealed the absence of a morphologically distinct floorplate in E9.5 *Shh* mutants, with the ventral region of the neural tube consisting instead of a thick epithelium (compare Fig. 2*j* with Fig. 2*k*; arrow). Notochord tissue is evident in cross-sections from caudal and some rostral axial levels in mutant embryos at this stage (see also Fig. 3).

Staining of bone and cartilage also revealed defects in the cranio-facial, axial and appendicular skeleton of *Shh* mutant embryos. Cranio-facial bones are severely affected and are almost entirely absent (Fig. 2*m*, *n*) despite the presence and nearly normal appearance of the branchial arches at E9.5 (Fig. 2*c*). Defects of the cranio-facial skeleton are commonly observed in association with neural tube defects, and in the case of *Shh* mutants these may be a secondary consequence of the extreme midbrain and forebrain defects. In the axial skeleton of *Shh* mutant embryos, most sclerotomal derivatives including the entire vertebral column are absent, with only five or six rib cartilages remaining. Other rib structures are difficult to assign in the absence of a vertebral column, but their cartilaginous composition suggests an anterior and ventral nature. In the appendages, distal structures are most affected, with a complete absence of digits and absence or fusion of the paired distal limb bones. Thus, in the hindlimb, which is more severely affected, the tibia and fibula are completely absent, although the femur is formed (Fig. 2*m*, *n*). In the forelimb, a bony extension of the humerus may represent either a fused ulna/radius or simply a long, bent humerus; these possibilities are difficult to distinguish given the absence of cartilage, which normally separates these bones at the elbow joint (Fig. 2*m*, *n*; arrow).

## Defective axial structures

Because notochord tissue seems to be present in caudal but not rostral cross-sections of E9.5 *Shh* mutant embryos, we sought to determine whether the notochord is established normally or displays defects at earlier stages. Fate mapping and transplant studies have shown that the regressing node is the primary source of notochord tissue during early embryonic development[23,24]. The *Brachyury* gene, which encodes a DNA-binding protein and is required for differentiation of the notochord, is normally expressed in the primitive steak and in the node and developing notochord of E7.5 and E8.5 embryos[25]. In E7.75 *Shh* mutant embryos, *Brachyury* gene expression appears normal, consistent with the presence of the node at this early stage of development

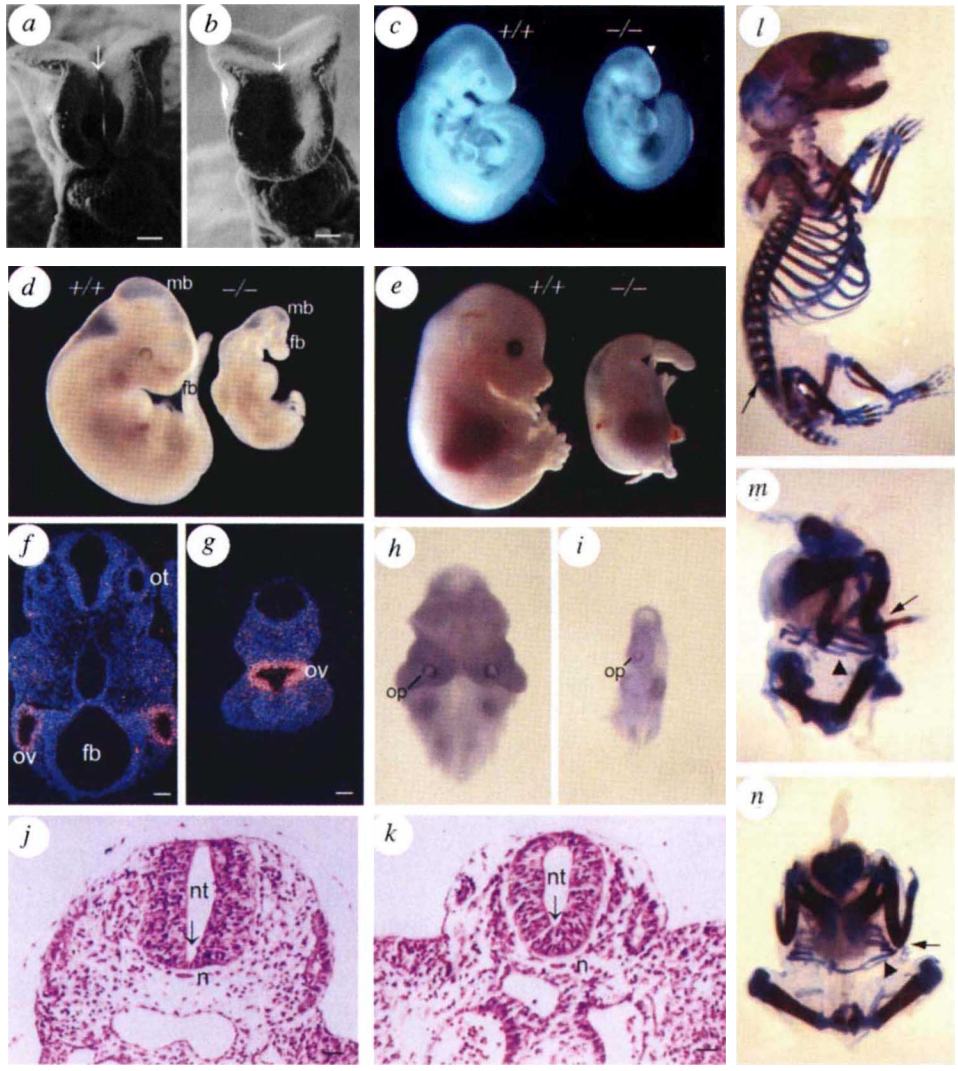


FIG. 2 Abnormal anatomy and histology of *Shh* mutant embryos. *a*–*e*, External morphology of wild-type (+/+) and mutant (−/−) embryos. *a*, *b*, Scanning electron micrographs of the rostral ends of E8.5 wild-type (*a*) and mutant (*b*) embryos; note the lack of a distinct midline (arrow) and the single continuous optic vesicle at the ventral midline of the mutant embryo. *c*, Lateral view of E9.5 embryos. An abnormal cephalic flexure and the apposition of ventral and dorsal neural tube surfaces is indicated by the arrowhead. *d*, Lateral view of E11.5 embryos. Note the reduction in overall size, the abnormal forebrain morphology, and the lack of bilateral eye structures in the mutant embryo. *e*, Lateral view of E15.5 embryos. At this stage the craniofacial region of the mutant embryo consists of a long proboscis, at the base of which is an accumulation of pigmented cells (arrowhead). Note the stunted limbs of the mutant, *f*, *g*, Cross-sections of E9.5 wild-type (*f*) and $Shh^{-/-}$ (*g*) embryos at the level of the optic vesicles hybridized with *micropthalmia* (*mi*) antisense RNA. Note the presence of a single *mi*-expressing optic vesicle in $Shh^{-/-}$ embryos. *h*, *i*, Facial view of whole-mount *in situ* hybridization with *Fgf8* antisense RNA to E10.5 wild-type (*h*) and $Shh^{-/-}$ (*i*) embryos. *Fgf8* expression highlights a single nasal pit forming within a single olfactory placode in the mutant embryo. *j*, *k*, Cross-sections at the level of the hind limb of wild-type (*j*) and $Shh^{-/-}$ (*k*) stained with haemotoxylin and eosin. Note the lack of a floorplate in the ventral midline of the mutant neural tube (arrow), despite the apparent presence of notochord tissue. *l*–*n*, Bone (brown) and cartilage (blue) stains of E18.5 wild-type (*l*) and $Shh^{-/-}$ embryos (*m*, *n*). In $Shh^{-/-}$ embryos, most of the sclerotomal derivatives such as spinal column (*l*, arrow) are missing with the exception of some rib cartilages (*m*, *n*, arrowhead). The distal limb structures are also missing; note the absence of cartilage at the elbow joint in the mutant (*m*, *n*, arrow). Abbreviations: fb, forebrain; mb, midbrain; n, notochord; nt, neural tube; op, olfactory placode; ov, optic vesicle; ot, otic vesicle. Scale bar, 100 μm. For comparison, mutant embryos in *m* and *n* are shown at 2.5-fold magnification relative to the wild-type in 1.

(data not shown). By E8.5, however, *Brachyury* gene expression becomes discontinuous in the rostral portion of mutant embryos (Fig. 3*a*). By E9.5, the rostral-most expression of the *Brachyury* gene is completely lost (Fig. 3*b*); this loss progresses in a rostral-to-caudal direction, as indicated by patchy *Brachyury* gene expression more caudally. The progressive, rostral-to-caudal loss of notochord tissue concomitant with loss of *Brachyury* gene expression suggests that *Shh* is required for the maintenance, but not the formation, of the notochord.

The *HNF-3β* gene, which encodes a winged-helix transcription factor required for development of the axial structures[26,27], is expressed in the node, developing notochord, head process, floorplate and gut endoderm, in a spatial pattern that is similar to but slightly precedes that of *Shh*[3]. At E7.75, although the localization of *HNF-3β* expression seems normal in *Shh* mutant embryos, the level of expression is consistently reduced in the notochord and in the head process (Fig. 3*c*). By E8.5, *HNF-3β* expression in axial mesoderm is completely absent (Fig. 3*d*), although gut expression persists for at least one more day of embryonic development (data not shown); expression of *HNF-3β* in the ventral neural tube of mutant embryos is never initiated. Initiation of *HNF-3β* expression in the ventral neural tube in normal embryos occurs before the stage at which the notochord degenerates in *Shh* mutant embryos; the failure to initiate *HNF-3β* expression in mutant neural tube thus suggests that Shh protein is the notochord-derived signal required for *HNF-3β* induction in the normal neural tube.

The notochord is also known to induce differentiation of other ventral cell types within the neural tube, including motor neurons[28]. The *Islet-1* gene (*Isl-1*) encodes a LIM homeodomain protein that is expressed in motor neurons, and mice lacking function of this gene fail to form motor neurons[29]. We therefore examined mutant embryos for the expression of Isl-1 protein as a marker for the presence of motor neurons. Normal expression of Isl-1 in the neural tube is first detected at E9.5 in a punctate pattern of nuclear staining lateral to the floorplate (Fig. 3*e*). In *Shh* mutant embryos, Isl-1 expression is absent in the neural tube at all axial levels (Fig. 3*f*), including caudal levels where the notochord persists. Failure to induce the Isl-1 marker even in the presence of the notochord suggests that Shh protein from the notochord may be required for differentiation of motor neurons. Alternatively, differentiation of motor neurons may require signalling from the floorplate, or from both the notochord and the floorplate.

## Dorsoventral pattern defects in the neural tube

Given the degeneration of the notochord and failure of the floorplate to develop in *Shh* mutant embryos, we examined dorsoventral (D–V) patterning of the neural tube at E11.5 by assaying the expression patterns of various *Pax* gene family members (reviewed in ref. 30). In the neural tube at the level of the prospective spinal cord, *Pax-3* is normally expressed in the alar palte, corresponding to the dorsal half of the neural tube (Fig. 4*a*).

*Pax-6*, in contrast, is expressed only weakly in the alar plate and more strongly throughout the basal plate except at the ventral midline (Fig. 4*c*). In *Shh* mutant embryos, high levels of *Pax-3* expression extend ventrally and across the midline where floorplate would normally be present (Fig. 4*b*). Similarly, expression of *Pax-6* also extends across the ventral midline in mutant embryos and is reduced to a level more characteristic of normal alar plate expression (Fig. 4*d*). In *Shh* mutant embryos, gene expression patterns in the ventral neural tube thus appear to lose the characteristics of normal basal plate (exclusion of *Pax-3*) and floorplate (exclusion of *Pax-6* from the midline) and acquire alar plate characteristics such as a high level of *Pax-3* expression and a reduced but uniform overall level of *Pax-6* expression. *Pax-2* expression, normally restricted to interneuronal regions of the alar and basal plates that lie adjacent to the sulcus limitans, also expands across the ventral midline in mutant embryos (Fig. 4*e*,*f*). The normal exclusion of *Pax-2* from dorsal parts of the neural tube is preserved, however, suggesting that dorsal pattern is maintained within *Shh* mutant embryos.

Because the notochord degenerates in *Shh* mutant embryos, the abnormal patterning of the ventral neural tube may be an indirect consequence of this loss rather than a direct consequence of loss of *Shh* function. To assess this possibility, expression of *Pax-3* within the E9.5 neural tube was examined in the caudal portion of mutant embryos where some notochord tissue is still present (compare Fig. 5*a* with Fig. 5*b*). The inability of notochord lacking *Shh* function to exclude *Pax-3* expression from the ventral portion of the neural tube, in conjunction with the results of ectopic expression[3,5,6,9,11–13] and explant studies[6,17,18,21], suggests a direct role for *Shh* in neural tube patterning.

## Patterning of paraxial mesoderm

Differentiation of the somite into dorsal dermatome, medial myotome and ventral sclerotome is mediated by inductive signals derived from surrounding tissues[31]. Previous studies have shown that *Shh* is capable of inducing expression of the ventral sclerotomal marker *Pax-1* and of suppressing the dorsal dermomyotomal marker *Pax-3*, either when expressed ectopically in the chick or when applied to presomitic mesoderm explants[15,16,20]. The expression of *Pax-3* normally is confined to the dermomyotome of the differentiating somite (Fig. 5*a*). In E9.5 mutant embryos *Pax-3* expression is ventrally expanded (Fig. 5*b*), suggesting that the sclerotome may also be affected. Surprisingly, we observed weak but reproducible *Pax-1* expression in E9.5 mutant somites (compare Fig. 5*c* with Fig. 5*d*), with a region of higher expression in a block of five or six somites (compare Fig. 5*e* with Fig. 5*f*). By E11.5 all somite expression of *Pax-1* is lost (Fig. 5*g*, *h*), indicating that *Shh* is essential for the maintenance, but not the initiation, of sclerotomal *Pax-1* expression.

The presence of skeletal muscle in later-stage *Shh* mutant embryos (data not shown) indicates that differentiation of myotomal derivatives does not require *Shh* function. However, at least two myotomal components have been resolved within the somite, the medial *myf-5*-expressing component and the lateral MyoD-expressing component (reviewed in ref. 32). We observed significantly reduced accumulation of *myf-5* transcripts at E9.5 (Fig. 5*i*, *j*) and normal levels of MyoD protein at E10.5 (Fig. 5*k*, *l*) throughout the axis of mutant embryos. These results are consistent with reports that medial but not lateral myotomal components are dependent on axial structures[33,34], and further suggests the possibility that *Shh* function contributes to this signal. As also observed for the *Pax-1* sclerotomal marker, however, *Shh* function appears not to initiate but to enhance or maintain expression of the *myf-5* lateral myotomal markers.

## Patterning of brain and eye

In comparison with their normal littermates, the brains of $Shh^{-/-}$ embryos are reduced in size, with progressively more severe morphological defects observed in the hindbrain, midbrain and forebrain. To characterize these abnormalities further we examined the expression in *Shh* mutant embryos of several homeobox genes that are expressed in restricted regions of normal E11.5 brain. In the normal forebrain, *Emx-1* expression[35] is restricted to the dorsal telecephalon corresponding to the neocortex (Fig. 6*a*). In *Shh* mutant embryos, *Emx-1* expression can be detected throughout a single vesicle present in the midline (Fig. 6*d*), suggesting that the normally bilateral lobes of the telencephalon are fused to form a single midline structure and that ventral forebrain structures are lost. Consistent with this interpretation, expression of the *Otx-2* gene[36] is also lost in ventral domains of the telencephalon and in the diencephalon (compare Fig. 6*b* with Fig. 6*e*); indeed, most of the diencephalon as an identifiable structure is absent in *Shh* mutant embryos. Reduced expression of *Otx-2* in the mesencephalon is also consistent with the reduction in size and the abnormal morphology of the midbrain in the *Shh* mutant (Fig. 6*e*). The deficit in the midbrain would appear to be in the anterior, as most of the remaining midbrain cells express the *En-2* gene[37], normally restricted to the posterior midbrain (compare Fig. 6*c* with Fig. 6*f*). Expression of the *En-2* gene at the isthmus is essentially normal, consistent with the presence of the midbrain/hindbrain constriction and also with the normal appearance of *Pax-2* expression at this constriction (data not shown). The expression in normal anterior/posterior sequence of *Emx-1*, *Otx-2* and *En-2* in prospective forebrain, midbrain and hindbrain domains suggests that the major requirement for *Shh* gene function is for ventral cell fate specification rather than anteroposterior patterning.

The vertebrate eye originates from evagination of the optic vesicles from the lateral walls of the forebrain (reviewed in ref. 38). After the optic vesicles have formed they undergo an additional invagination to form double-layered cups that differentiate into a neural retina and a pigmented epithelium; these cups remain connected to the diencephalon by the optic stalks. In *Shh* mutant embryos the optic vesicles are fused at the midline and the optic stalks are deficient or absent. There is no invagination to form the characteristic double-layered optic cups, and the fused eye tissue at the midline forms a pigmented epithelium with no apparent differentiation of retinal tissue (Fig. 2*f*, *g*). To analyse eye patterning defects in mutant embryos further we examined the expression patterns of *Pax-6*, *Otx-2* and *Pax-2* genes in the E11.5 mutant eye. *Pax-2* and *Pax-6* have been shown to play important roles during eye development (reviewed in ref. 38) and serve as early markers for proximal cells that contribute to the future optic stalk, and for distal cells that contribute to both layers of the optic cup[9,13], respectively. The expression of *Pax-6* throughout most of the normal optic cup, including the pigmented epithelium and the neural retina, is shown in Fig. 6*g*. *Pax-6* expression occurs throughout the cyclopic mutant eye structure (Fig. 6*j*), which is constituted solely of pigmented epithelium. *Otx-2* expression similarly persists in the cyclopic *Shh* mutant eye (Fig. 6*h*, *k*). The expression of *Pax-2*, normally restricted to the optic stalks connecting the eye primordia to the brain (Fig. 6*i*), is absent in *Shh* mutant embryos (Fig. 6*l*), consistent with the histologically apparent absence of the optic stalk and the loss of ventral forebrain structures.

## Discussion

**Roles of *Shh* expression in neural patterning and notochord maintenance.** One of the early functions of the notochord is to induce differentiation of ventral cell types such as floorplate cells and motor neurons in the overlying neural ectoderm. Our studies demonstrate, however, that, despite the presence of a differentiated notochord during early stages of development, floorplate cells and motor neurons are not induced in *Shh* mutants. Conversely, in other vertebrate mutants, such as the zebrafish *floating heat* (*flh*) mutant[39], or the murine *Brachyury* (T) mutant[25] and its zebrafish homologue *no tail* (*ntl*)[40], floorplate cells develop in rostral portions of the embryo despite the absence of a differentiated notochord. These notochord mutants, however, express *Shh* in presumptive notochord precursor cells in the midline. Expression of *Shh* in the absence of definitive notochord

differentiation may therefore be sufficient for ventral neural patterning, whereas notochord differentiation in the absence of *Shh* function is not. Together with the results of neural plate explant studies[6,17,18,21], these results suggest that ventral patterning by the *Shh* signal can operate independently of notochord development.

Our finding that *Shh* is not essential for node formation or for notochord differentiation is not surprising, as expression of *Shh* in the node is first detectable at the late streak to early head-fold stages, by which time a morphologically recognizable node and notochord are already present. The requirement for *Shh* in maintenance of the notochord, however, represents a previously

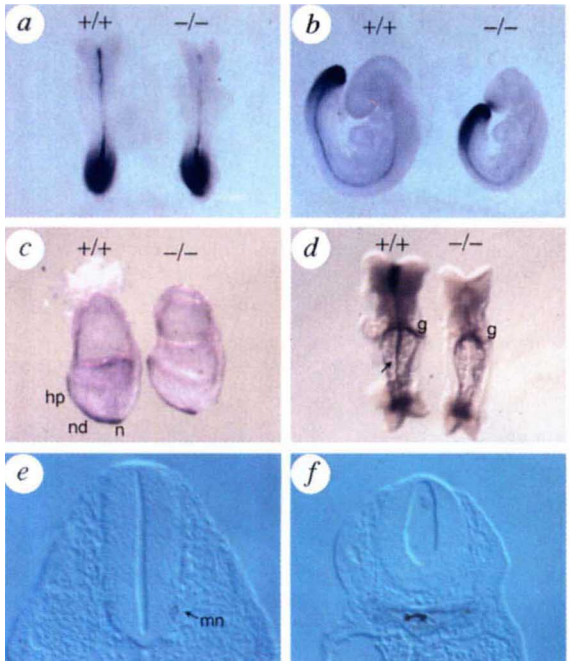


FIG. 3 Defective axial structures in *Shh* mutant embryos. *a*, *b*, Expression of *Brachyury* in E8.5 (*a*) and 9.5 (*b*) embryos. Note the discontinuity and loss of *Brachyury* expression in the rostral part of *Shh* mutant (−/−) embryos. *c*, *d*, Expression of HNF-3β expression in the node (n), notochord (nd) and head process (hp) of $Shh^{-/-}$ embryos is similar to the normal pattern, although the level of expression is reduced. At E8.5 (*d*, ventral view), HNF-3β expression in the floorplate and the notochord (arrow) is completely absent, although expression persists in the gut (g). *e*, *f*, Cross-sections through E9.5 wild-type (*e*) and $Shh^{-/-}$ (*f*) embryos at the level of the forelimbs labelled with Islet-1 antibody. Accumulation of Islet-1 protein in the motor neurons (mn, arrow) can be detected as bilateral punctate staining within the ventrolateral portion of the normal neural tube (*e*). This staining is completely absent in $Shh^{-/-}$ embryos (*f*).

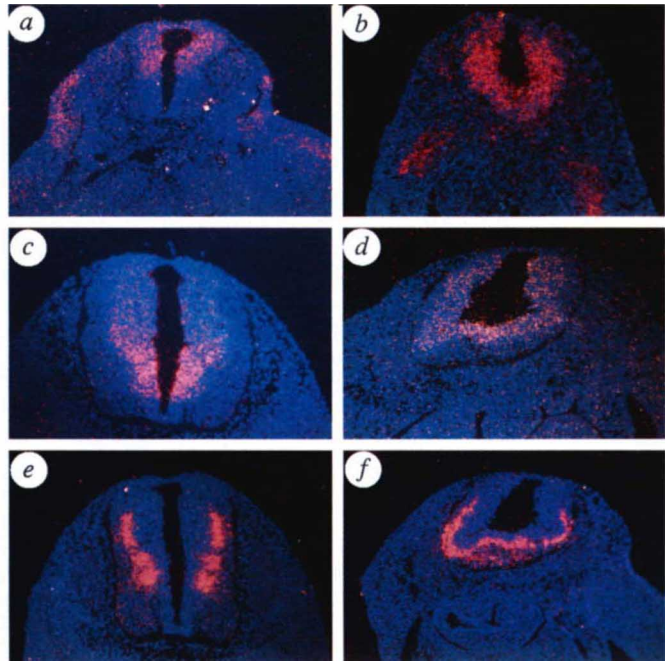


FIG. 4 Dorsoventral patterning defects in the neural tube of *Shh* mutant embryos. *a*–*f*, Cross-sections through E11.5 wild-type (*a*, *c*, *e*) and $Shh^{-/-}$ (*b*, *d*, *f*) embryos hybridized with $^{33}$P-labelled antisense RNAs. *a*, *b* *Pax-3* is normally expressed in the alar plate of the neural tube (*a*) but in $Shh^{-/-}$ (*b*) expression expands across the ventral midline of the neural tube. *c*, *d*, *Pax-6* expression, normally high in the basal plate and weak in the alar plate (*c*), is distributed uniformly throughout the neural tube including the ventral midline at a reduced level characteristic of normal alar plate expression (*d*). *e*, *f*, Normal *Pax-2* expression is restricted to the interneuron region flanking the sulcus limitans (*e*) but in $Shh^{-/-}$ mutants it expands across the ventral midline of the neural tube (*f*). Note the exclusion of *Pax-2* expression from the dorsal midline in both wild-type and mutant embryos. Scale bar, 100 μm.

FIG. 5 Somite development in $Shh^{-/-}$ embryos. *a*–*d*, Cross-sections of wild-type (*a*, *c*) and $Shh^{-/-}$ (*b*, *d*) E9.5 embryos showing somite expression of *Pax-3* (*a*, *b*) and *Pax-1* (*c*, *d*). Normal expression of *Pax-3* in the dermomyotome (dm) is ventrally expanded in $Shh^{-/-}$ embryos and *Pax-1* expression is reduced. *e*–*h*, Whole-mount E9.5 (*e*, *f*) and E11.5 (*g*, *h*) embryos showing *Pax-1* expression in wild-type (*e*, *g*) and $Shh^{-/-}$ (*f*, *h*) mutant embryos. Relative to wild type, the reduced level of *Pax-1* sclerotome expression in the E9.5 mutant (*f*) is completely lost by E11.5 (*h*), whereas forelimb expression is largely normal (asterisks). *i*, *j*, Whole-mount E9.5 wild-type (*i*) and $Shh^{-/-}$ (*j*) embryos showing expression of *myf-5* RNA. *k*, *l*, E10.5 wild-type (*k*) and $Shh^{-/-}$ (*l*) embryos showing MyoD protein accumulation in the myotome (arrows). MyoD protein expression in $Shh^{-/-}$ mutant embryos is similar to that in wild type, but expression of *myf-5* RNA in mutant embryos is significantly reduced. Abbreviations: br, branchial arches; dm, dermomyotome; sc, sclerotome.

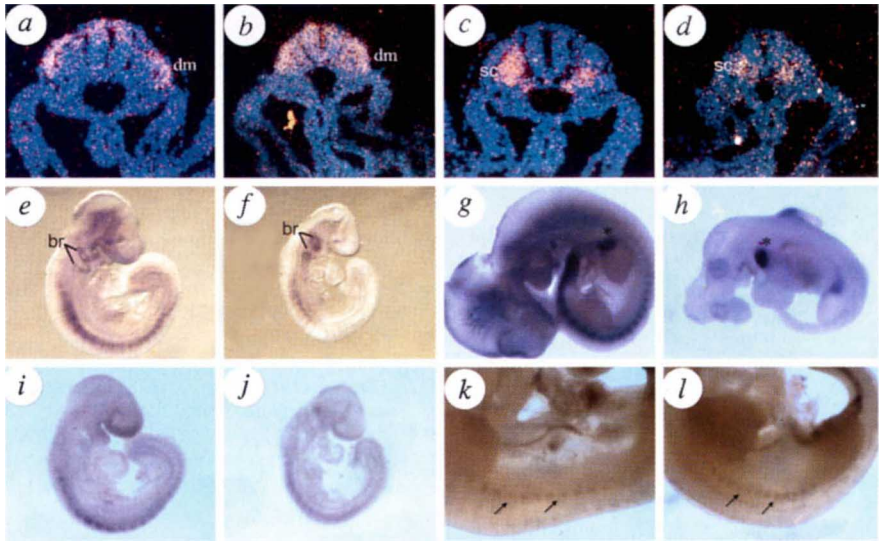

unforeseen role. This maintenance function may represent an autocrine action of the *Shh* signal produced within the notochord. Alternatively, notochord maintenance may require signals derived from other tissues, such as the floorplate, whose formation is dependent on earlier *Shh* function; this possibility seems unlikely, however, given the persistence of notochord in *cyclops* mutants of the zebrafish, which lack floorplate cells[41], and in chick embryos from which the neural tube has been extirpated before floorplate formation[33].

**Regulatory interactions in axial tissues.** Analysis of the *Shh* mutant phenotype revealed several features of the regulatory interactions between genes expressed in axial tissues. Previous studies had suggested the existence of a positive feedback between the *Shh* signal and the transcription factor *HNF-3β* for mutual maintenance of expression in the neural tube. We have found here that *Shh* is indeed required for the later *HNF-3β* expression, but our analysis also shows that early expression of *HNF-3β* in the axial mesoderm of late streak to early head-fold stages is initiated independently of *Shh* function. Regulation of *HNF-3β* expression thus changes from early independence to a later requirement for *Shh* function.

Another example of changing regulatory relationships in axial structures is the shift of *Brachyury* gene expression from early dependence on *HNF-3β* function[26,27] to later independence, as indicated by our observation in the *Shh* mutant that *Brachyury* gene expression persists considerably longer than expression of *HNF-3β*. Previous studies have suggested that the maintenance of *Brachyury* expression in the notochord is mediated through autoregulation[42]. Alternatively, maintenance of *Brachyury* expression could involve mouse homologues of genes such as *flh*, whose function is required for *ntl* expression in zebrafish[39].

The developmental logic underlying these dynamically changing regulatory relationship seems to be an early marshalling of axial gene expression under the regulatory control of the HNF-3β transcription factor (or perhaps other transcription factors acting upstream). Once expression of axial genes is established, *Shh* and *HNF-3β* expression become mutually interdependent and expression of both genes is established in the ventral midline of the neural tube through the signalling action of the Shh protein. Restriction of other early axial genes such as *Brachyury* to expression in the notochord is accomplished by uncoupling expression from *HNF-3β* regulatory input, and possibly by an increasing reliance on auto-regulation or regulation by other notochord-specific genes such as *flh*.

**The role of *Shh* in development of the axial skeleton.** Shh protein has been implicated as the notochord-derived signal responsible for induction of the sclerotome[15,16,20], and the reduced level of *Pax-1* expression and the absence of most sclerotomal derivatives in $Shh^{-/-}$ embryos suggest a role for *Shh*. Furthermore, the observed skeletal defects in $Shh^{-/-}$ embryos overlap with those of *Pax-1* null embryos, in which ventral portions of the vertebrae, such as vertebral bodies, intervertebral discs and a few medial portions of the ribs, are missing[43]. Nevertheless, some expression of *Pax-1* occurs in the absence of *Shh* function, indicating that *Shh* is not absolutely required *in vivo* for specification of sclerotomal cell fates. The role of *Shh* thus might be to maintain or expand the population of committed sclerotome cells. Consistent with this view is the observation that *Shh* protein is a potent mitogen for presomitic explants[20], and that low levels of *Pax-1* are expressed in these explants even in the absence of induction by notochord or Shh protein[16]. The absence of the entire vertebral column in $Shh^{-/-}$ embryos, as opposed to a partial loss in *Pax-1* mutant embryos, suggests that sclerotome-promoting effects of *Shh* may involve modulation of other genes in addition to *Pax-1*; one such gene could be *Pax-9*, which is expressed in the sclerotome and has an expression pattern similar to that of *Pax-1* (ref. 44).

**The role of *Shh* in limb development.** Based on the initial view of *Shh* and the zone of polarizing activity in anteroposterior limb patterning, an early prediction might have been that loss of *Shh* function would lead simply to anterior/posterior mispatterning of

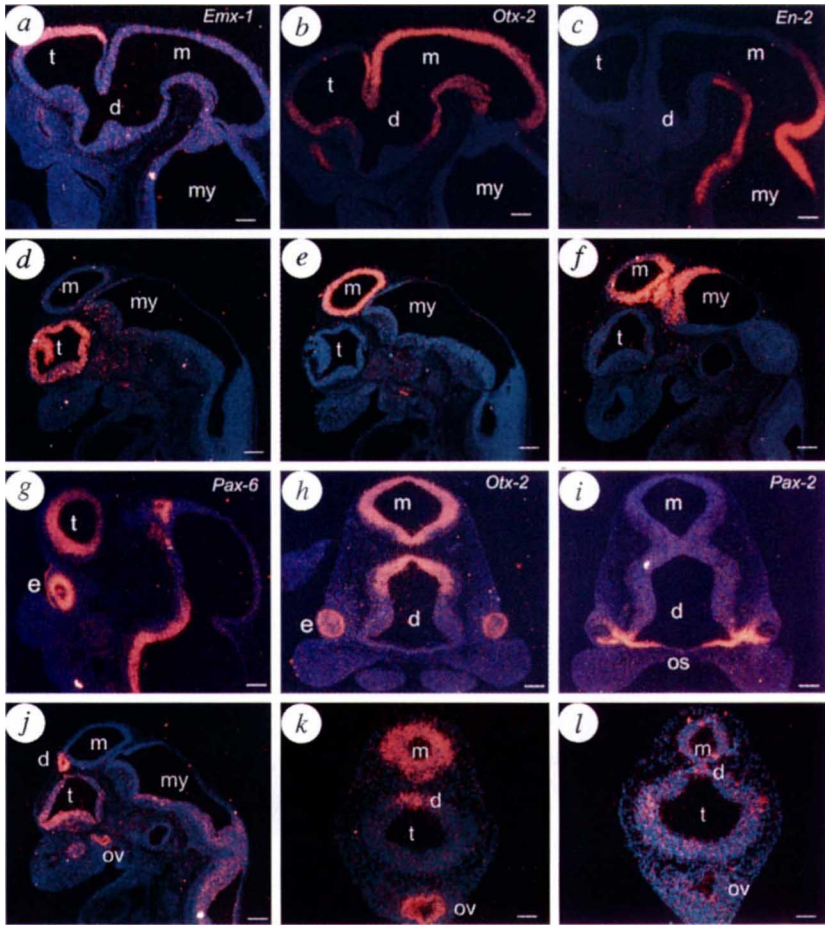


FIG. 6 Brain and eye patterning defects in *Shh* mutant embryos. *a–f*, Parasagittal sections of E11.5 wild-type (*a–c*) and $Shh^{-/-}$ (*d–f*) embryos. *a*, *d*, Expression of *Emx-1* is normally restricted to the dorsal telencephalon (*a*). In the $Shh^{-/-}$ embryo, *Emx-1* expression can be detected throughout a single telencephalic vesicle located at the midline (*d*). *b*, *e*, Normal expression of *Otx-2* in the ventral telencephalon (*b*) is absent in $Shh^{-/-}$ embryos (*e*). *c*, *f*, *En-2* expression marks the midbrain/hindbrain boundary, which is present in $Shh^{-/-}$ embryos. *g–l*, Parasagittal (*g*), midsagittal (*j*) and coronal (*h*, *i*, *k*, *l*) sections through the eye of E11.5 wild-type (*g–i*) and $Shh^{-/-}$ (*j–l*) embryos. *g*, *j*, *Pax-6* expression is retained in the single optic vesicle present in $Shh^{-/-}$ embryos. *Pax-6* is also expressed in the remnant of the dorsal diencephalon of $Shh^{-/-}$ embryos. *h*, *k*, *Otx-2* is expressed in the midbrain, the remnant of the dorsal diencephalon, and the single optic vesicle of $Shh^{-/-}$ embryos. Arrow indicates the floorplate in the normal mesencephalon, which is absent in $Shh^{-/-}$ embryos. *i*, *l*, The optic stalks and *Pax-2* expression are absent in $Shh^{-/-}$ embryos. Abbreviations: d, diencephalon; e, eye; m, mesencephalon; my, myelencephalon; ov, optic vesicle; os, optic stalks; t, telencephalon. Scale bar in *a–j*, 100 μm; in *k*, *l*, 35 μm.

the limbs[4]. The dramatic loss of distal structures observed here, however, indicates that *Shh* plays an important role in promoting distal limb fates. Consistent with such a role for *Shh*, experimental amputations of posterior portions of chick limb buds produced dramatic losses of distal structures[45]. These distal truncations resemble those observed in *Shh* mutant mice, and are far more severe than defects caused by anterior amputations of comparable extent. One possible link between the distal truncations caused by posterior limb-bud amputation and loss of *Shh* function is the apparent role for fibroblast growth factor (FGF) signals in limb outgrowth and the requirement for *Shh* in maintenance of FGF-4 expression in the posterior apical ectodermal ridge[46] (C.C. *et al.*, manuscript in preparation). Normal expression of *Shh* at the posterior margin of the limb bud is thus implicated in dynamically shaping limb pattern during outgrowth, presumably through a fairly local induction of cell proliferation, with distal structures deriving largely from the postaxial region of the limb bud[47].

**The role of *Shh* in establishing the ventral midline of the brain and spinal cord.** Throughout the neural tube, loss of *Shh* function results in failure to establish cell fates and gene expression patterns characteristic of the ventral midline. Perhaps the most striking defects in *Shh* mutant embryos occur in the forebrain and its derivatives, which at E11.5 consist of a single fused telencephalic vesicle that overlies a single fused optic vesicle situated at the base of an externally apparent proboscis. This phenotype is reminiscent of a spectrum of human congenital malformations referred to collectively as holoprosencephaly, which in its most severe form is accompanied by cyclopia, a single nasal chamber, a single telencephalic vesicle, and other forebrain and facial midline defects[48]. An extensive review of cyclopia and associated developmental malformations raised the key question of whether the eye anlage in the early rostral neural plate is normally single and continuous or instead is bilaterally divided[49,50], and concluded that the early eye field is continuous across the midline and that later subdivision of this single eye field at the midline depends on influences from prechordal plate mesoderm. These conclusions were based on elegant experiments involving *in vivo* culture of median or lateral strips form rostral neural plate, either alone or recombined with underlying prechordal mesoderm or prechordal plate mesoderm. Also consistent with these conclusions is the induction of cyclopia by the removal of prechordal plate mesoderm from beneath the early neural plate of amphibian embryos (reviewed in refs 49, 50).

Our study is consistent with the idea that *Shh* expression in prechordal plate mesoderm contributes to the signal that establishes the ventral midline of the brain and subdivides the eye field. The expression of *Shh* is normally first detected in the prechordal mesoderm underlying the rostral neural plate of mouse embryos at the midstreak stage[3,7]. In the early head-fold stage of $Shh^{-/-}$ embryos, *HNF-3β* and *Brachyury* expression appear normal, indicating that the prechordal plate mesoderm is present during early embryogenesis. Rostral neural plate defects are morphologically apparent shortly thereafter, suggesting that, as observed for spinal cord regionalization and morphogenesis, it is the absence of the *Shh* signal rather than absence of axial mesoderm that is responsible for patterning defects. With regard to eye patterning, we have demonstrated that *Shh* is required for *Pax-2* expression and for optic stalk formation in the forebrain. These results are consistent with previous evidence from zebrafish studies suggesting that *hh* activity from the ventral midline normally stimulates expression of *Pax-2* in the adjacent optic stalk precursors and represses expression of *Pax-6*, thus restricting *Pax-6* expression and its associated retinal and epithelial fates to distal portions of the optic vesicle[9,13]. These effects of *Shh* signalling identify a molecular pathway by which bilateral subdivision of the eye field at the midline might be accomplished while simultaneously imposing a proximo-distal patterning influence on the developing optic vesicle. □

## Methods

**Targeted recombination of the *Shh* gene.** The targeting vector was constructed by inserting a 14-kb *Sal*I (*Sal* sites were vector-derived) fragment of *Shh* genomic DNA into the *Xho*I site of a thymidine kinase-containing vector. To delete the *Shh* exon 2 region, the 3.0-kb *Xba*I/*Xho*I fragment was replaced with the *Xba*I/*Sal*I fragment containing the Pgk-neo cassette. The final targeting vector was linearized at a unique *Xho*I site before use in the transfection of ES cells. R1 ES cells were grown, transfected and subjected to double selection[26,51]. Homologous recombinant ES clones were identified by Southern analysis and further analysed using PCR primers specific to *Shh* exon 2 and to the *neo* gene to confirm the absence of exon 2 sequences in the disrupted gene. Frozen cells were expanded and used for injection into C57Bl/6J blastocysts. The primers were: P1, 5′-GACCATGTCTGCACACTTAGGTTCC-3′; P2, 5′-GAAGGCC AGGAGGAGAAGGCTCAC-3′; P3, 5′-CTGTGCTCGACGTTGTCACTG-3′; P4, 5′-GATCCCCTCAGAAGAACTCGT-3′.

**Histology and *in situ* detection of RNA and protein expression.** Embryos were fixed in 4% paraformaldehyde overnight at 4 °C, dehydrated, embedded in paraplast, and sectioned at 5 μm. Sections were stained with haematoxylin and eosin for histological analysis. Cartilage and bones were stained with alcian blue and alizarin red[43]. *In situ* hybridization to tissue sections[7] and *in situ* hybridization to whole embryos were performed[26]. Whole-mount immunohistochemistry using Islet-1 antibody was performed essentially as described[29]. After immunostaining, embryos were sectioned at 5 μm.

Received 9 July; accepted 23 August 1996.

1. Nüsslein-Volhard, C. & Wieschaus, E. *Nature* **287,** 795–801 (1980).
2. Lee, J. J., von Kessler, D. P., Parks, S. & Beachy, P. A. *Cell* **71,** 33–50 (1992).
3. Echelard, Y. *et al. Cell* **75,** 1417–1430 (1993).
4. Riddle, R. D., Johnson, R. L., Laufer, E. & Tabin, C. *Cell* **75,** 1401–1416 (1993).
5. Krauss, S., Concordet, J.-P. & Ingham, P. W. *Cell* **75,** 1431–1444 (1993).
6. Roelink, H. *et al. Cell* **76,** 761–775 (1994).
7. Chang, D. T. *et al. Development* **120,** 3339–3353 (1994).
8. Ekker, S. C. *et al. Development* **121,** 2337–2347 (1995).
9. Ekker, S. C. *et al. Curr. Biol.* **5,** 944–955 (1995).
10. Lopez-Martinez, A. *et al. Curr. Biol.* **5,** 791–796 (1995).
11. Ruiz i Altaba, A., Jessell, T. M. & Roelink, H. *Mol. Cell. Neurosci.* **6,** 106–121 (1995).
12. Lai, C.-J., Ekker, S. C., Beachy, P. A. & Moon, R. T. *Development* **121,** 2349–2360 (1995).
13. Macdonald, R. *et al. Development* **121,** 3267–3278 (1995).
14. Hammerschmidt, M., Bitgood, M. J. & McMahon, A. P. *Genes Dev.* **10,** 647–658 (1996).
15. Johnson, R. L., Laufer, E., Riddle, R. D. & Tabin, C. *Cell* **79,** 1165–1173 (1994).
16. Fan, C.-M. & Tessier-Lavigne, M. *Cell* **79,** 1175–1186 (1994).
17. Roelink, H. *et al. Cell* **81,** 445–455 (1995).
18. Marti, E., Bumcrot, D. A., Takada, R. & McMahon, A. P. *Nature* **375,** 322–325 (1995).
19. Hall, T. M. T., Porter, J. A., Beachy, P. A. & Leahy, D. J. *Nature* **378,** 212–216 (1995).
20. Fan, C.-M. *et al. Cell* **81,** 457–465 (1995).
21. Hynes, M. *et al. Neuron* **15,** 35–44 (1995).
22. Hodgkinson, C. A. *et al. Cell* **74,** 395–404 (1993).
23. Lawson, K. A., Meneses, J. J. & Pedersen, R. A. *Development* **113,** 891–911 (1991).
24. Beddington, R. S. *Development* **120,** 613–620 (1994).
25. Herrmann, B. G. *et al. Trends Genet.* **10,** 280–286 (1994).
26. Ang, S. L. & Rossant, J. *Cell* **78,** 561–574 (1994).
27. Weinstein, D. C. *et al. Cell* **78,** 575–588 (1994).
28. Yamada, T., Pfaff, S. L., Edlund, T. & Jessell, T. M. *Cell* **73,** 673–686 (1993).
29. Pfaff, S. L., Mendelsohn, M., Stewart, C. L., Edlund, T. & Jessell, T. M. *Cell* **84,** 309–320 (1996).
30. Mansouri, A., Stoykova, A. & Gruss, P. *J. Cell Sci. (suppl.)* **18,** 35–42 (1994).
31. Christ, B. & Ordahl, C. P. *Anat. Embryol.* **191,** 381–396 (1995).
32. Cossu, G., Tajbakhsh, S. & Buckingham, M. *Trends Genet.* **12,** 218–223 (1996).
33. Rong, T. M., Teillet, M.-A., Ziller, C. & Le Douarin, N. M. *Development* **115,** 657–672 (1992).
34. Christ, B., Brand-Saberi, B., Grim, M. & Wilting, J. *Anat. Embryol.* **186,** 505–510 (1992).
35. Boncinelli, E., Gulisano, M. & Broccoli, V. *J. Neurobiol.* **24,** 1356–1366 (1993).
36. Simeone, A. *et al. EMBO J.* **12,** 2735–2747 (1993).
37. Joyner, A. L. & Martin, G. R. *Genes Dev.* **1,** 29–38 (1987).
38. Macdonald, R. & Wilson, S. W. *Curr. Opin. Neurobiol.* **6,** 49–56 (1996).
39. Talbot, W. S. *et al. Nature* **378,** 150–157 (1995).
40. Halpern, M. E., Ho, R. K., Walker, C. & Kimmel, C. B. *Cell* **75,** 99–111 (1993).
41. Hatta, K., Kimmel, C. B., Ho, R. K. & Walker, C. *Nature* **350,** 339–341 (1991).
42. Herrmann, B. G. *Development* **113,** 913–917 (1991).
43. Wallin, J. *et al. Development* **120,** 1109–1121 (1994).
44. Neubuser, A., Koseki, H. & Balling, R. *Dev. Biol.* **170,** 701–716 (1995).
45. Hinchliffe, J. R. & Gumpel-Pinot, M. *J. Embryol. Exp. Morphol.* **62,** 63–82 (1981).
46. Cohn, M. J. & Tickle, C. *Trends Genet.* **12,** 253–257 (1996).
47. Sordino, P. & Duboule, D. *Trends Ecol. Evol.* **11,** 114–119 (1996).
48. Fitz, C. R. *Neuroimag. Clin. N. Am.* **4,** 263–281 (1994).
49. Adelmann, H. B. *Q. Rev. Biol.* **11,** 116–182 (1936).
50. Adelmann, H. B. *Q. Rev. Biol.* **11,** 284–304 (1936).
51. Nagy, A., Roswant, J., Nagy, R., Abramow-Newerly, W. & Roder, J. C. *Proc. Natl Acad. Sci. USA* **90,** 8424–8428 (1993).

ACKNOWLEDGEMENTS. H.W. and P.A.B. are senior co-authors. We thank J. Gearhart and D. Bol for a 129 ES cell genomic library; A. Nagy and J. Rossant for R1 ES cells; M. Capecchi for the thymidine kinase-containing vector; P. Soriano for *Pgk-neo*; and Syntex Discovery Research for gancyclovir; E. Boncinelli, H. Sasaki, B. Hogan, B. G. Herrmann, H. Arnheiter, P. Gruss, T. Jessell, A. Joyner, G. Dressler and G. Martin for probes; K. Cveklova for help in tail DNA preparation; V. Tanner for help with scanning electron microscopy; and C.-M. Fan, M. Halpern and O. Sundin for criticism of this manuscript. P.A.B. is an investigator of the Howard Hughes Medical Institute.

CORRESPONDENCE should be addressed to C.C. (e-mail: chiangc@dir6. nichd.nih.gov) or P.A.B. (e-mail: phil.beach@qmail.bs.jhu.edu), and requests for materials to H.W. (e-mail: hw@helix.nih.gov) or P.A.B.